Small-angle x-ray scattering measurements of hydrogen evolution from an epitaxial Nb film

Brent J. Heuser, Monica M. C. Allain, and W. C. Chen*
University of Illinois, Department of Nuclear, Plasma, and Radiological Engineering, Urbana, Illinois 61801
(Received 9 April 2002; published 23 October 2002)

Small-angle x-ray scattering (SAXS) measurements have been performed to investigate particle morphology during *in situ* hydrogen evolution from a 1000-Å epitaxial Nb film on $(11\bar{2}0)$ sapphire initially loaded to saturation with hydrogen. The SAXS intensity follows the plate or disk single-particle form factor (Q^{-2}, where Q is the wave-vector transfer) during hydrogen evolution. A fit to this power-law behavior yields a plate thickness of ≈7 Å. A second power-law behavior (Q^{-3}) was observed after complete hydrogen evolution. This power law corresponds to the small-angle scattering response from edge dislocations and is consistent with the broadening of the lattice mosaic induced by hydride decomposition.

DOI: 10.1103/PhysRevB.66.155419 PACS number(s): 61.10.Eq, 68.35.Dv, 68.35.Rh, 68.55.Ln

Small-angle scattering measurements of thin films in transmission geometry are difficult with conventional x-ray sources because of attenuation within the substrate material. We have taken advantage of the high brilliance of an insertion-device beam line at the Advanced Photon Source to perform such a measurement. Of particular interest to us is the evolving microstructure associated with hydride phase transformations, either during formation or decomposition. The study of hydrogen in bulk metals now spans three centuries. On the other hand, interest in hydrogen-metal thin-film systems dates to the 1980s.[1–4] Much of the most recent thin-film work has relied on x-ray diffraction (XRD) to investigate lattice strain as a function of hydrogen gas pressure.[5–7] Lattice strain measurements do not, however, provide information regarding the particle morphology. As demonstrated in this work, small-angle x-ray scattering (SAXS) can provide particle morphology information of a precipitating phase in thin-film geometry.

Nb grows nearly strain free on $(11\bar{2}0)$ or *a*-plane sapphire under molecular-beam epitaxy growth conditions with the following orientation relationship between the sapphire and Nb lattice: $[11\bar{2}0]\|[110]$, $[0001]\|[111]$, $[\bar{1}100]\|[11\bar{2}]$.[8] The 1000-Å-thick Nb film investigated here was grown at a substrate temperature of 800 °C, a growth rate of 0.33 ML/sec, and a pressure that did not exceed 1×10^{-9} Torr. The epitaxial quality of the film was confirmed with XRD (see below). The film was capped with a 40-Å-thick Pd layer (grown at room temperature to prevent interdiffusion) to facilitate hydrogen absorption and desorption. The $(11\bar{2}0)$ sapphire substrate was cut with a 0.05° miscut, polished to 5-Å RMS roughness, and was 0.5 mm thick. The XRD measurements were performed at the University of Illinois Frederick Seitz Materials Research Laboratory using a Philips XPert diffractometer with Cu $K\alpha$ radiation (x-ray wavelength of 1.540 56 Å). The angular resolution of this instrument is 0.003°. The SAXS measurements were performed using the BESSRC-CAT ID-12 beam line at the Advanced Photon Source at Argonne National Laboratory. The SAXS incident x-ray beam energy was 12.0 keV, corresponding to a wavelength of 1.04 Å, and the data were recorded over a wave-vector transfer or Q range of 0.02 to 0.7 $Å^{-1}$. This Q range [Q is given by $Q=(4\pi/\lambda)\sin\theta$, where λ is the wavelength and θ is half the scattering angle] corresponds to a length scale range of ≈10–300 Å. The SAXS measurements were performed with the film downstream of the substrate. SAXS data presented here are radial averages over all azimuthal angles recorded by the two-dimensional detector.

The room-temperature SAXS response of the Nb film before and after hydrogen loading, along with the open beam measurement, are shown in Fig. 1. This film had not been exposed to hydrogen prior to the Fig. 1 measurement. The Nb film was loaded with hydrogen *ex situ* at 100 °C by exposure to 100 Torr of H_2 gas, and then allowed to cool to room temperature before evacuation of the H_2 gas. These loading conditions are sufficient to completely transform bulk Nb to the α' phase.[9] While the hydrogen-metal phase behavior is perturbed by thin-film geometry, we believe these

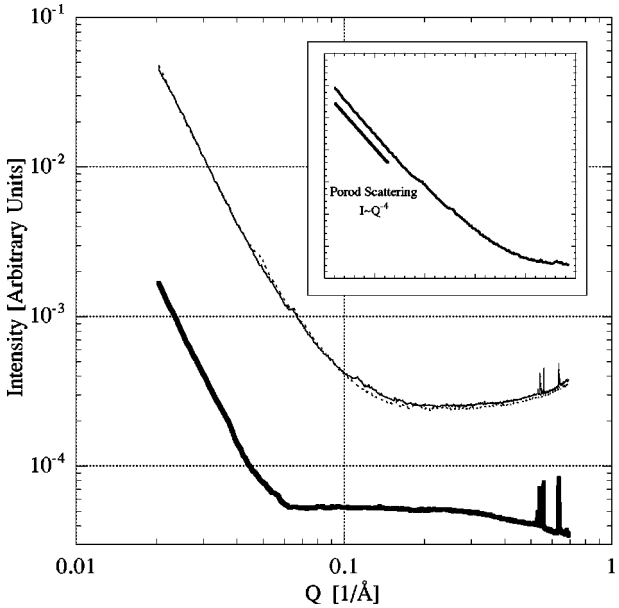

FIG. 1. Response of the open beam (thick solid line), room-temperature prehydrogen Nb film (dotted line) and room-temperature hydrogen-loaded Nb film (thin solid line). The inset shows the net scattering response (prehydrogen minus open beam) in ln-ln format over the same Q range. The net response follows the Porod law at lowest Q. The spikes in the data at high Q are an artifact of the detector.

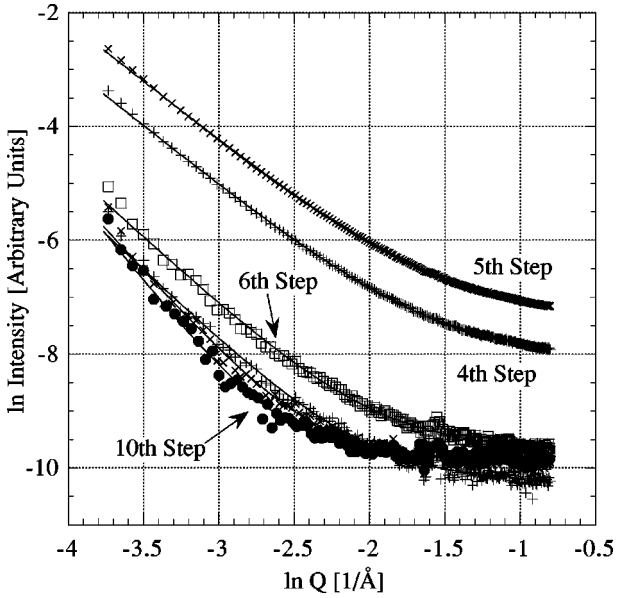

FIG. 2. The net SAXS response recorded during hydrogen evolution as the Nb film was heated *in situ* from room temperature to 200 °C (see text for details). The room-temperature hydrogen-loaded measurement was subtracted to determine the net response. Every other heating step is shown for clarity. The two unlabeled curves are the second and eighth heating steps.

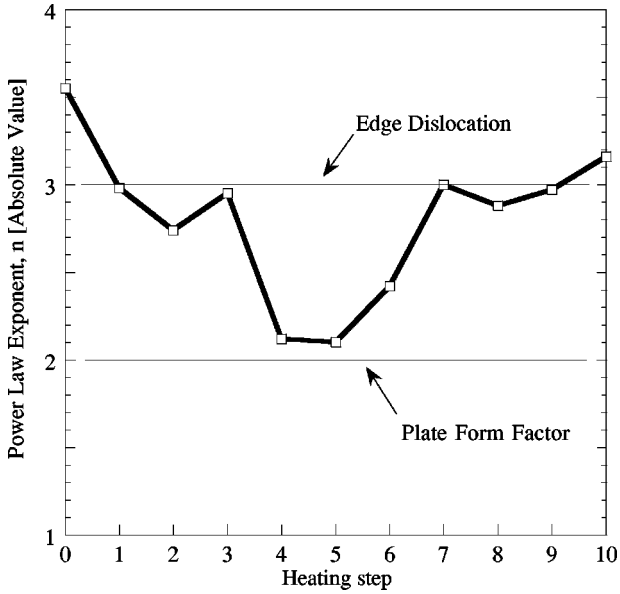

FIG. 3. The variation of the power-law exponent n during hydrogen evolution for all heating steps. A $n=2$ power law is observed at the peak of the SAXS response (fifth heating step), indicating the formation of plates. The equilibrium response after complete hydrogen evolution (seventh heating step on) is characterized by a $n=3$ power law. This is the response from an orientation average of an edge dislocation.

loading conditions saturated epitaxial Nb as well. This is based on neutron reflectivity measurements of polycrystalline thin-film Nb (Ref. 10) and the initial SAXS response, as discussed presently. Notice two aspects of the Fig. 1 data. First, the net response of the unloaded film (Fig. 1 inset) follows the Porod law,[11] $I \sim Q^{-4}$. Porod scattering results from abrupt changes in the electron density associated with internal or external surfaces. Rough external surfaces, such as the unpolished surface of the sapphire substrate opposite the film, will induce a measurable Porod response. The second important aspect of the Fig. 1 data is the very small net signal of the loaded film relative to the unloaded film. This indicates that the film was completely transformed to the α' phase during hydrogen loading; nonuniformity within the loaded film would result in larger scattered intensities, as was observed during hydrogen evolution.

A significant temperature hysteresis exists in the thin-film Nb-H system and hydrogen does not evolve at room temperature. It is for this reason that the Nb film could be loaded *ex situ* without hydrogen loss. The Nb film was heated *in situ* to 200 °C under vacuum to evolve hydrogen and induce the α' to α decomposition reaction. The temperature was measured with a thermocouple embedded in the sample holder. The SAXS response was recorded for 10 sec every 30 sec during the 5-min heating ramp (at 36° per minute) from room temperature to 200 °C. The evolution of the net SAXS response during this heating ramp is shown in Fig. 2. These data are fit with a power law, $I \sim Q^{-n}$, where n is the power-law exponent. Power-law exponents for all heating steps are shown in Fig. 3. The power-law exponent equals 2 at the peak of the SAXS response (fourth and fifth heating steps in Fig. 2). This is the power law of a dilute mixture of plates or disks; in other words, the single-particle form factor of a plate or disk.[11] A $n=3$ power law is observed at the end of the heating ramp. This is the small-angle scattering response from edge dislocations.[12] The uncertainty in n determined from the fits shown in Fig. 2 are a few percent at most. The most important comparison in Fig. 3 is the $n=2$ value at the peak of the scattering intensity and the $n=3$ response at the end of the heating ramp. The fits to the data readily resolve this difference.

The film was held at 200 °C for 1 h after the heating ramp to confirm that the α' to α decomposition reaction was complete. No measurable change was observed in the SAXS response. The film was then heated to 250 °C and held for an additional hour. A measurable net Porod response was observed at 250 °C relative to the 200 °C measurement (not shown). However, this response was less than 2% of the response at the fifth heating step (and ≈3% of the Porod scattering shown in the Fig. 1 inset) and cannot represent small-angle scattering from additional α' decomposition. We can therefore state with certainty that the $n=3$ response at the end of the heating ramp was not influenced by a residual α' phase.

The net SAXS responses from the fifth heating step and the equilibrium measurement at 200 °C are shown in Fig. 4. The fifth heating step curve, after an additional background subtraction, is fit with the complete single-particle form factor for a plate,[11]

$$I(Q) = \frac{A}{Q^2} \exp\left(\frac{-Q^2T^2}{12}\right), \tag{1}$$

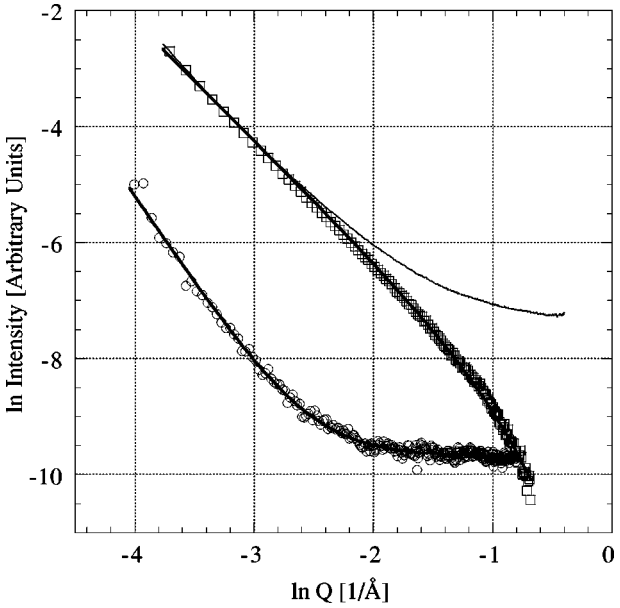

FIG. 4. Comparison of the fifth heating step net response (solid line) and the 200-°C equilibrium net response (open circles). The fifth heating step data after additional background subtraction (open boxes) are fit with the complete single-particle form factor for a plate, yielding a plate thickness of 7 Å. The 200-°C net response is fit with the edge dislocation cross section plus a constant background term.

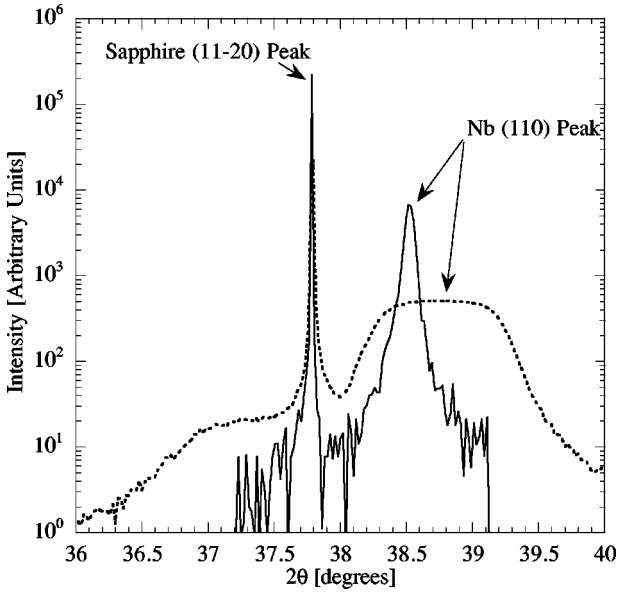

FIG. 5. Specular scans of the prehydrogen (solid line) and cycled, posthydrogen (dotted line) Nb film. The considerable broadening of the posthydrogen Nb(110) peak is due to a reduction in the out-of-plane coherence length, not strain broadening.

where A is a constant and T is the plate thickness. The effect of the exponential term is revealed after background subtraction and influences the data at the highest Q (roll over above 0.21/Å). The fit of Eq. (1) yields a plate thickness of 7 Å. The equilibrium SAXS response after hydrogen evolution is well fit with a Q^{-3} edge dislocation power law. The Q^{-3} scattering law was developed analytically as an orientation average over all directions about an edge dislocation.[12] The azimuthally averaged data in Fig. 4 represents such an orientation average.

Dislocation formation is known to accompany incoherent hydride formation and decomposition in bulk Nb.[13,14] The edge dislocation SAXS response after hydrogen evolution is consistent with the hydride formation-decomposition cycle leading to a loss of structural coherency via dislocation formation within the epitaxial Nb film. Structural coherence of a thin film can be characterized with XRD specular and rocking scans. In a specular scan the wave-vector transfer is perpendicular to the film surface, while the scan direction is parallel to the film surface in a rocking curve measurement. Specular and rocking curve peak widths are inversely proportional to the out-of-plane and in-plane coherence lengths, respectively. A perfect lattice extending over macroscopic distances in three dimensions—in other words, a lattice with infinite coherence lengths—will have peak widths equal to the Darwin width (on the order of 10 arc sec). In this case, the measured peak widths will be given by a convolution of the crystal lattice Darwin width and the resolution of the diffractometer. The out-of-plane coherence length of an epitaxial thin film cannot be greater than the film thickness, and the peak width in a specular scan is broadened by this finite-size effect. The in-plane coherence length is not constrained by the film thickness and is a measure of the epitaxial quality of the film. Films with excellent epitaxial quality will accordingly have rocking curve peak widths that are determined by the above-mentioned convolution. Typically, at least for heteroepitaxial metal films, the rocking curve will have this as a narrow component plus a broad component. The former corresponds to the portion of the film with perfect in-plane registration or epitaxy (that is, commensurate with the perfect substrate). The latter corresponds to the portion of the film that has lost, at least partially, perfect registration and is no longer commensurate with the substrate.

Specular scans of the Nb film before hydrogen exposure and after hydrogen evolution are shown in Fig. 5. Two prominent features are seen in the prehydrogen specular scan; the sapphire $(11\bar{2}0)$ peak, with a full width at half maximum (FWHM) nearly equal to the instrumental resolution, and the Nb(110) peak. The FWHM of the Nb peak is 0.08° (on the 2θ scale), corresponding to an out-of-plane coherence length of 1080 Å (approximately equal to the film thickness). The out-of-plane strain associated with the angular position of the Nb(110) peak in the specular scan is -1.5×10^{-3}. In other words, the Nb lattice is in slight compression normal to the film surface compared to bulk Nb. This is the Poisson response of the film to an in-plane tensile strain state. Hydrogen cycling induces noticeable broadening of the Nb(110) peak (FWHM is ~1°). A reduction of the out-of-plane coherence length to ≈90 Å is associated with this broadening. Also notice that the Nb(110) peak has shifted to a higher 2θ angle after hydrogen cycling. The out-of-plane strain associated with this shift is -7×10^{-3}. Large residual compressive strains have been observed in hydrogen-cycled polycrystalline Nb multilayer systems,[6,15] but not in single-layer epitaxial Nb films to our knowledge.

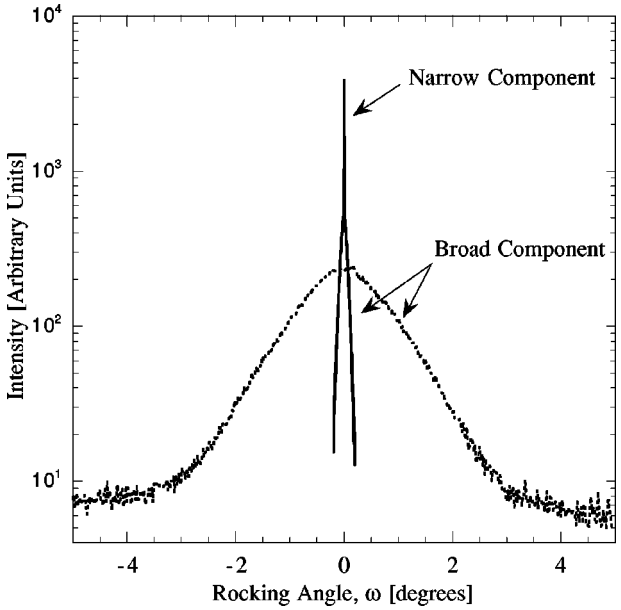

FIG. 6. Rocking curves of the prehydrogen (solid line) and posthydrogen (dotted line) Nb(110) peak. The prehydrogen rocking curve has both a narrow and broad component, as expected from an epitaxial metal film (see text). The posthydrogen curve does not have a narrow component, signaling a complete loss of structural coherency.

The shape of the cycled, posthydrogen Nb(110) peak in Fig. 5 appears to be unusually broad and flat. The two possible sources of this shape are strain broadening and lattice mosaic broadening. The former represents a variation in the lattice spacing about some nominal value, while the latter represents a variation in the angular tilt of the lattice planes. The one-dimensional slice through the post-hydrogen Nb(110) reciprocal lattice point cannot distinguish between the two sources. A two-dimensional map can; isointensity contours are oval shaped for a mosaic broadened reciprocal lattice point, but develop sharp, pointy features when strain broadening exists. A two-dimensional map (not shown) clearly demonstrated that significant mosaic broadening occurred in the posthydrogen sample.

The rocking curves through the Nb(110) reflection are shown in Fig. 6. The prehydrogen curve exhibits both a narrow and broad component. The FWHM of the broad component is 0.1° (700 Å coherence length), a reasonable value for epitaxial Nb on *a*-plane sapphire. As discussed above, hydrogen cycling has induced significant broadening of the Nb(110) rocking curve. The narrow component has been completely eliminated and the FWHM of the broad component is over 2°. This broadening arises from dislocation-induced lattice tilting. The corresponding in-plane coherence length is 20 Å.

One relevant point of discussion concerns the regions of the film that are coherent with the substrate. The epitaxial or interfacial dislocation network in the Nb-sapphire epitaxial system has been resolved with transmission electron microscopy analysis.[8,16] This work demonstrates that the in-plane lattice mismatch of Nb(110) on a-plane sapphire can be entirely accommodated with an array of misfit edge dislocations. The local lattice strain and lattice tilt associated with the individual dislocations in this array accounts for the measured FWHM and coherence length of the *broad* component of the prehydrogen rocking curve. Regions of the Nb lattice, again before hydrogen cycling, between the individual dislocations are coherent with the substrate and give rise to the resolution-limited narrow component of the rocking curve. It is important to note that the size of these coherent regions is small, on the order of the misfit dislocation spacing (25 or 140 Å for our case).[16] However, many of these regions remain in registry with the perfect substrate over microns and this results in a narrow rocking curve component of a few thousandths of a degree.

The SAXS and XRD data establish a clear description of hydride decomposition in epitaxial Nb. As in bulk Nb, phase separation proceeds via plate formation with concomitant dislocation generation. A plate thickness of 7 Å appears to imply a coherent α phase as the maximum scattering intensities were recorded in our measurements. However, the plate form factor does not carry in-plane dimensional information. The only requirement is that the scattering objects have a platelike shape. It is likely that the particles forming during the decomposition reaction have aspect ratios of order five to ten, leading to a loss of at least partial coherency in the plane of the plates. The distortion of the Nb lattice after hydrogen cycling is evident in the XRD data; both in-plane and out-of-plane coherence lengths are reduced to very small values compared to the prehydrogen case. This reduction of film coherency is the result of dislocation formation, as seen in the SAXS response after complete hydrogen evolution.

This work was supported by the National Science Foundation under Grant No. DMR-9982520. The XRD measurements were performed at the Center for Microanalysis of Materials at the FS-MRL, University of Illinois, which is supported by the U.S. DoE under Grant No. DEFG02-91-ER45439. The SAXS experiments were carried out at the APS BESSRC-CAT, which is supported by the U.S. DoE under Contract No. W-31-109-ENG-38. The authors would like to acknowledge the assistance of Dr. M. Sardela (FS-MRL UIUC) and Dr. S. Seifert (APS ANL) for help with XRD and SAXS, respectively. In addition, the Nb film was grown at the UIUC EpiCenter by Dr. C. Durfee (Intel) while he was a member of Professor C. P. Flynn's research group and this is gratefully acknowledged.

*Present address: NIST Center for Neutron Research, National Institute of Standards and Technology, Gaithersburg, MD 20899.

[1] G. Alefeld and J. Völkl, *Hydrogen in Metals I* (Springer, Berlin, 1978).

[2] Y. Fukai, *The Metal-Hydrogen System* (Springer, Berlin, 1993).

[3] P. F. Miceli, H. Zabel, J. A. Dura, and C. P. Flynn, J. Mater. Res. **6**, 964 (1991).

[4] D. E. Azofeifa and N. Clark, Z. Phys. Chem. (Munich) **181**, 387 (1993).

[5] G. Song, M. Geitz, A. Abromeit, and H. Zabel, Phys. Rev. B **54**, 14 093 (1996).
[6] Q. M. Yang, G. Schmitz, S. Fähler, H. U. Krebs, and R. Kirchheim, Phys. Rev. B **54**, 9131 (1996).
[7] F. Klose, Ch. Rehm, M. Fieber-Erdmann, E. Holub-Krappe, H. J. Bleif, H. Sowers, R. Goyette, L. Tröger, and H. Maletta, Physica B **283**, 184 (2000).
[8] G. Gutekunst, J. Mayer, and M. Rühle, Philos. Mag. A **75**, 1329 (1997).
[9] J. F. Smith, Bull. Alloy Phase Diagrams **4**, 39 (1983).
[10] A. E. Munter, B. J. Heuser, and M. W. Ruckman, Phys. Rev. B **55**, 14 035 (1997).
[11] G. Porod, in *Small Angle X-Ray Scattering*, edited by O. Glatter and O. Kratky (Academic, London, 1982).
[12] A. K. Seeger, J. Appl. Phys. **30**, 629 (1959).
[13] T. Schober, Phys. Status Solidi A **30**, 107 (1975).
[14] B. J. Heuser and J. W. Althauser, J. Phys.: Condens. Matter **9**, 8945 (1997).
[15] C. Borchers, U. Laudahn, A. Pundt, S. Fähler, H. U. Krebs, and R. Kirchheim, Philos. Mag. A **80**, 543 (2000).
[16] G. Gutekunst, J. Mayer, V. Vitek, and M. Rühle, Philos. Mag. A **75**, 1357 (1997).